

Full-Range and Rapid-Tracking Carrier Phase and Frequency Estimator for 16-QAM Coherent Systems

Adaickalavan Meiyappan, Pooi-Yuen Kam, and Hoon Kim

Department of Electrical & Computer Engineering, National University of Singapore, 4 Engineering Drive 3, Singapore 117576

E-mail: elekampy@nus.edu.sg

Abstract: We present a carrier phase and frequency estimator for 16-QAM with frequency acquisition range of ± 0.5 times the symbol rate, speed of 15 times faster than differential frequency estimation, and robustness in tracking time-varying frequency.

OCIS codes: (060.4510) Optical communications; (060.1660) Coherent communications

1. Introduction

Capacity increase to service the sustained growth of data traffic with a constrained utilizable bandwidth demands a spectrally-efficient multilevel modulation format. The 16 quadrature amplitude modulation (QAM) with coherent detection is a promising approach with integrated 16-QAM modulators already being developed [1] and recent 16-QAM coherent system demonstrations in [2] and [3]. Performance of 16-QAM is highly sensitive to the frequency offset, Δf , between the transmitter and local oscillator lasers, when left uncompensated [4]. Decision-directed phase-locked loop (DD-PLL) was employed in [2] and [3] for carrier recovery but the permissible frequency offset was constrained to 100 and 50 MHz, respectively, to ensure reliable frequency locking. However, tunable lasers can have a frequency error of up to ± 2.5 GHz [5] leading to a possible frequency offset of 5 GHz. In general, optimization of DD-PLL parameters is difficult and its performance is very poor at large frequency offsets [6].

Two prevalent frequency estimators in the literature are the fast Fourier transform based estimator (FFTbE) and the differential frequency estimator (DiffFE), which have been adapted for 16-QAM in [7] and [4], respectively. FFTbE requires a computationally prohibitive solution involving a 2-step process, which includes locating the peak in the periodogram of the received signal raised to its 4th power. In DiffFE, consecutive Class I symbols (innermost and outermost rings) are phase differenced and raised to the 4th power. The frequency estimation range of both FFTbE and DiffFE is limited to $\pm R/8$ due to their 4th power operation, where R is the symbol rate.

We recently derived a least-squares-based joint carrier phase and frequency offset estimator termed complex-weighted, decision-aided, maximum-likelihood carrier estimator (CW-DA-ML CE) in [8] for M -ary phase-shift keying (MPSK) signals. In this paper, we extend CW-DA-ML CE to non-constant envelope 16-QAM systems and show that it achieves near-ideal, unbiased, frequency estimation range of $\pm R/2$ regardless of laser linewidth. Furthermore, we prove CW-DA-ML CE's rapid frequency acquisition, which is 15 times faster than that of DiffFE in 16-QAM, and its robustness in tracking real-life time-varying frequency offset without the aid of pilot sequence.

2. Operating principle of CW-DA-ML CE

The discrete-time received sample for the k th symbol after digital equalization, assuming ideal symbol timing, is: $r(k) = m(k)\exp[j(\omega k + \theta(k))] + n(k)$. Here, $m(k)$ is the k th data symbol, $\omega = 2\pi\Delta fT$ is the angular frequency (T = symbol duration), and $\theta(k)$ is the phase noise modeled as zero-mean Gaussian random walk with temporal correlation $E[\theta(i)\theta(j)] = 2\pi\Delta\nu T \cdot \min[i, j]$, where $\Delta\nu$ is the combined laser linewidth. The $n(k)$ is a zero-mean additive white Gaussian noise. By exploiting the temporal correlation of phase noise over the immediate past L signals, a reference phasor (RP) is formed in a transversal filter manner: $V'(k+1) = C(k)\mathbf{w}^T(k)\mathbf{y}(k)$, where $\mathbf{w}(k) = [w_1(k) \cdots w_L(k)]^T$ is a complex filter-weight vector and $\mathbf{y}(k) = [r(k)\hat{m}^*(k) \cdots r(k-L+1)\hat{m}^*(k-L+1)]^T$ is the filter-input vector with its data modulation removed using the complex conjugate of the receiver's decision, $\hat{m}^*(l)$. Each received signal in $\{r(k+1), r(k), \dots, r(k-L+1)\}$ experiences a corresponding angular frequency offset of $\{\omega(k+1), \omega k, \dots, \omega(k-L+1)\}$ which reduces the correlation among filter inputs and degrades the accuracy of RP. Hence, we introduced $\mathbf{w}(k)$ to rotate all of $\{r(k), \dots, r(k-L+1)\}$ to the same angular frequency offset as $r(k+1)$ which is $\omega(k+1)$, thereby effectively removing the frequency offset effect in the filter. To adapt RP to a non-constant-envelope QAM constellation, we introduce the factor $C(k) = 1/\sum_{l=1}^L |\hat{m}(k-l+1)|^2$ to normalize the magnitude of $V'(k+1)$ to ~ 1 , thus making CW-DA-ML CE applicable to any arbitrary modulation format. Finally, the angle of RP is the estimate of $\omega(k+1) + \theta(k+1)$. Ideally $\mathbf{w}(k) = [\exp(j\omega) \cdots \exp(j\omega L)]^T$, but ω is unknown in practice. Utilizing the method of least squares, we chose $\mathbf{w}(k)$ adaptively at each time k to minimize a sum-of-error-squares cost function: $J(k) = \sum_{l=1}^k |r(l)/\hat{m}(l) - C(l-1)\mathbf{w}^T(k)\mathbf{y}(l-1)|^2$. Minimizing $J(k)$, we obtain $\mathbf{w}(k) = \Phi^{-1}(k)\mathbf{z}(k)$, where $\Phi^{-1}(k)$ is an L -by- L autocorrelation

matrix and $\mathbf{z}(k)$ is an L -by-1 cross-correlation vector. Note that $C(k)$ is not necessary in MPSK format and CW-DA-ML reduces to the classic DA-ML CE of [9] when $\mathbf{w}(k) = [1 \ \dots \ 1]^T$.

3. Results and discussion

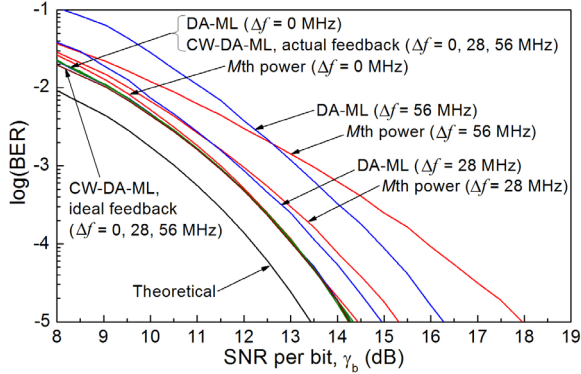


Fig. 1. BER of M th power, DA-ML, and CW-DA-ML CE.

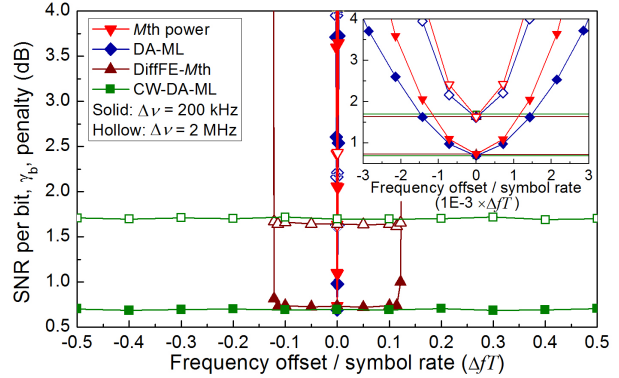


Fig. 2. Penalty vs frequency offset. Inset shows $\Delta f T = [-3, 3] \times 10^{-3}$.

Performance of CW-DA-ML CE with filter length $L = 10$ in a differentially-encoded 112 Gbit/s single polarization 16-QAM signal is evaluated through Monte Carlo simulations. Bit-error rate (BER) performance of CW-DA-ML CE is compared against that of DA-ML using $L = 10$ [9] and block M th power CE using $L = 20$ [10], at laser linewidth of 500 kHz in Fig. 1. As the frequency offset increases from 0 to 28 and 56 MHz, the signal-to-noise ratio (SNR) per bit, γ_b , penalty at $\text{BER} = 10^{-4}$ for M th power CE increases by 0.8 and 2.9 dB, respectively. Likewise, DA-ML CE incurs 0.5 and 1.85 dB penalty. On the other hand, CW-DA-ML CE ($\Delta f = 0, 28, 56$ MHz) replicates the BER performance of DA-ML CE ($\Delta f = 0$) over the entire SNR range tested, incurring no additional SNR penalty and thus demonstrating its near-ideal frequency estimation. Fig. 1 also shows that the performance loss of CW-DA-ML CE with actual, compared to ideal, decision feedback is negligible for BER below 10^{-2} .

Fig. 2 plots the SNR penalty with respect to coherent 16-QAM at $\text{BER} = 10^{-4}$ at two representative extremes of commercially available laser linewidths, $\Delta \nu$, of 200 kHz (e.g., external cavity laser) and 2 MHz (e.g., distributed feedback laser). Block M th power [10], DA-ML [9], and the DiffFE followed by block M th power scheme (termed as DiffFE- M th) proposed in [4] are also plotted for reference in Fig. 2. DiffFE- M th CE uses $L = 20$ and a received sample size of $N = 40000$ for frequency estimation. CW-DA-ML CE achieves a complete, unbiased, frequency offset estimation range of $\pm R/2$ and is operable regardless of laser linewidth, albeit with increased SNR penalty at higher laser linewidths.

Total phase-plus-frequency error variance against the received sample size, N , used for frequency estimation is plotted in Fig. 3 for CW-DA-ML and DiffFE- M th CE at $\gamma_b = 14$ dB and $\Delta f = 2.8$ GHz. For CW-DA-ML CE, N represents the number of received samples over which the complex weight vector is updated and after which the weight vector is kept constant. The error variance decreases initially due to improving frequency estimate accuracy but reaches an error floor limited by the value of laser phase noise. Contrary to intuition, the error variance of CW-DA-ML CE reaches the error floor within $N = 1000$ at higher laser linewidth of 2 MHz, much faster than the $N =$

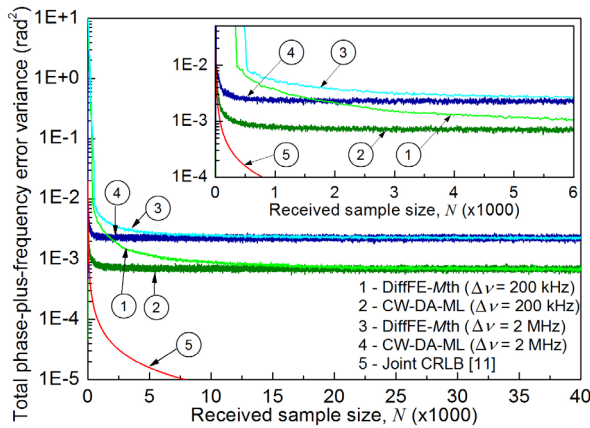


Fig. 3. Error variance vs received sample size in DiffFE- M th and CW-DA-ML CE. Inset shows enlarged $N = [0, 6] \times 10^3$.

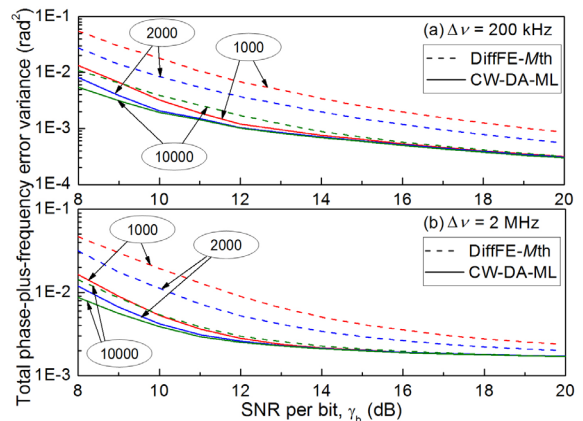


Fig. 4. Accuracy of DiffFE- M th and CW-DA-ML CE at different N (indicated inside oval) and a $\Delta \nu$ of (a) 200 kHz, or (b) 2 MHz.

2000 required at lower laser linewidth of 200 kHz. The frequency estimate accuracy attainable is limited by the laser linewidth, thus a lower N is sufficient to reach the lower accuracy allowed at higher laser linewidths. Error variance of DiffFE- M th converges to that of CW-DA-ML CE at $N = 15000$ and 30000 at laser linewidth of 2 MHz and 200 kHz, respectively. Therefore, CW-DA-ML CE is 15 times faster than DiffFE- M th in frequency acquisition. Furthermore, the initial degree of decay of error variance in CW-DA-ML CE follows closely that of the joint Cramer-Rao lower bound (CRLB) for constant phase and frequency offset estimation [11], reiterating the rapid frequency acquisition feature of CW-DA-ML CE in the presence of laser phase noise.

Fig. 4 illustrates the error variance against SNR at $\Delta f = 2.8$ GHz and different values of N . CW-DA-ML CE's superior or equal error variance as DiffFE- M th CE at a given N and SNR can be ascribed to the following two reasons. First, extensive simulations indicate that on average, 1 pair of consecutive Class I symbols occur for every 4 transmitted symbols in 16-QAM. Thus, DiffFE- M th CE only uses about $N/2$ samples whereas CW-DA-ML uses all N samples for frequency estimation. Second, DiffFE- M th CE only uses a 1-sample lag autocorrelation whereas CW-DA-ML CE uses up to L -sample lag autocorrelation which is more resilient to additive noise and thus improves the frequency estimate. The latter reason leads to CW-DA-ML CE's better error variance than DiffFE- M th CE at lower SNR region. We remark that CW-DA-ML CE does not experience sharp SNR threshold but rather a gradual one where its error variance deteriorates slowly with decreasing SNR. As the gradual SNR threshold is a decreasing function of N , CW-DA-ML CE can operate at low SNR by increasing the sample size N appropriately.

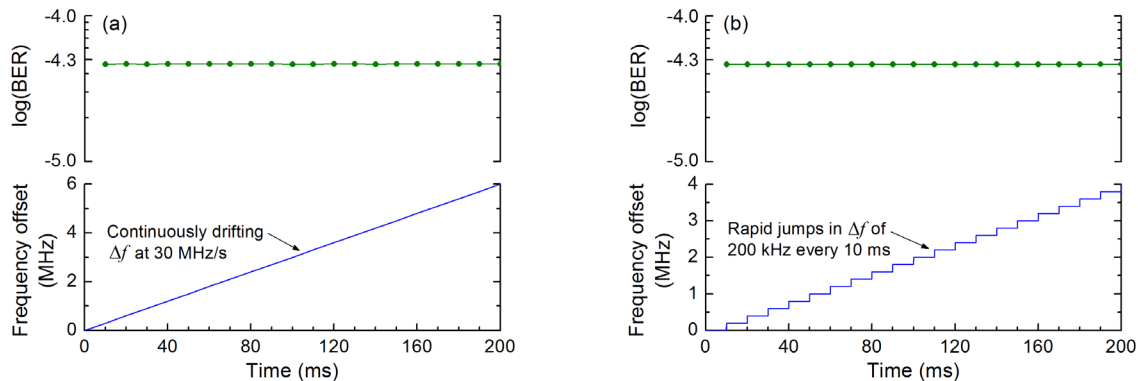


Fig. 5. BER of CW-DA-ML CE in time-varying frequency offset: (a) continuous drift, and (b) rapid jumps.

In practice, frequency offset can continuously drift in the range of MHz/s due to temperature or aging and also experience sudden jumps due to mechanical disturbances or vibrations to the laser. We demonstrate CW-DA-ML CE's robustness in tracking a frequency offset experiencing continuous drift of up to 30 MHz/s and rapid jumps of up to 200 kHz every 10 ms, which are simulated in Fig. 5(a) and (b), respectively, at $\Delta\nu = 500$ kHz and $\gamma_b = 13.5$ dB. The stable BER about 4.6×10^{-5} , measured over 10ms intervals, demonstrates the reliable tracking of time-varying frequency offset without the aid of pilots. Larger frequency jumps can be tracked provided the jumps are less frequent. CW-DA-ML CE can respond to changing channel conditions because it has an observation $\{r(l), 0 \leq l \leq k\}$ dependent cost function $J(k)$, negligible error propagation, and rapid frequency acquisition.

4. Conclusions

We have presented a viable joint carrier phase and frequency estimator for practical systems. It is applicable to all PSK and QAM formats, achieves frequency estimation range of ± 0.5 times the symbol rate, acquires frequency offset 15 times faster than differential frequency estimator, operable at low SNR, and can track real-life time-varying frequency offset without the need for pilots.

5. References

- [1] C. R. Doerr et al., "28-Gbaud InP square or hexagonal 16-QAM modulator," in Proc. OFC/NFOEC 2011, paper OMU2.
- [2] P. J. Winzer et al., "Spectrally efficient long-haul optical networking using 112-Gb/s ...," J. Lightw. Technol. **28**, 547-556 (2010).
- [3] T. Kobayashi et al., "160-Gb/s polarization-multiplexed 16-QAM long-haul transmission ...," in Proc. OFC/NFOEC 2010, paper OTuD1.
- [4] I. Fatadin and S. J. Savory, "Compensation of frequency offset for 16-QAM ...," IEEE Photon. Technol. Lett. **23**, 1246-1248 (2011).
- [5] "Integrable Tunable Laser Assembly Multi Source Agreement," Optical Internetworking Forum, OIF-ITLA-MSA-01.1, Nov. 22 2005.
- [6] K.-Y. Kim and H.-J. Choi, "Design of carrier recovery algorithm for high-order QAM with large ...," in Proc. ICC 2001, pp. 1016-1020.
- [7] M. Selmi et al., "Accurate digital frequency offset estimator for coherent PolMux QAM ...," in Proc. ECOC 2009, paper P3.08.
- [8] A. Meiyappan et al., "A complex-weighted, decision-aided, maximum-likelihood carrier phase ...," Opt. Express **20**, 20102-20114 (2012).
- [9] P.-Y. Kam, "Maximum likelihood carrier phase recovery for linear suppressed-carrier ...," IEEE Trans. Commun. **34**, 522-527 (1986).
- [10] I. Fatadin et al., "Laser linewidth tolerance for 16-QAM coherent optical systems ...," IEEE Photon. Technol. Lett. **22**, 631-633 (2010).
- [11] M. P. Fitz, "Planar filtered techniques for burst mode carrier synchronization," in Proc. GLOBECOM'91, pp. 365-369.